EFFECT OF PRESSURE ENVIRONMENT ON THE

DAMPING OF VIBRATING STRUCTURES

David G. Stephens and Maurice A. Scavullo

NASA Langley Research Center
Langley Station, Hampton, Va.

Presented at the 34th Symposium on Shock, Vibration,
and Associated Environments

Monterey, California
October 13-15, 1964

EFFECT OF PRESSURE ENVIRONMENT ON THE

DAMPING OF VIBRATING STRUCTURES

By David G. Stephens[*] and Maurice A. Scavullo[*]
NASA Langley Research Center

ABSTRACT

29495

An investigation was conducted to determine the mechanism of the air

damping exhibited by rigid bodies of different shapes oscillating in a pressure

environment. Circular and rectangular panels, as well as a sphere and cylinder,

were attached to cantilever springs and the free decay of an induced oscilla-

tion measured at pressure levels from atmospheric to 4×10^{-2} torr. Data are

presented to show the effect of pressure, vibratory amplitude, shape, and sur-

face area on the air damping of the models. Results indicate that the magnitude

of the air damping may greatly exceed the structural damping of the system. The

air damping associated with the panels is directly proportional to the pressure

and amplitude which is indicative of dissipative loads proportional to the

dynamic pressure. Furthermore, the panel damping was found to be independent

of shape, and a nonlinear function of the surface area. The sphere and cylinder

exhibit viscous damping characteristics which are in good agreement with avail-

able theory.

INTRODUCTION

The vibratory response of a mechanical system is greatly influenced by the

presence of damping. In most situations this damping results from the dissipa-

tion of energy in such forms as internal hysteresis, interface or joint fric-

tion, and external or air damping. This latter form of damping is highly

---

[*]Aerospace Engineer.

dependent upon the magnitude of the pressure environment and, therefore, deserves particular attention in studying the response of systems designed to operate throughout a wide range of pressure. If, for example, the vibration tests of a space vehicle are conducted under atmospheric pressure conditions, the damping level and consequently the response will be somewhat different than in the actual operating environment which involves reduced pressures. Thus in interpreting and extrapolating the results of such tests, one must understand and treat the effect of the pressure environment on the results.

The purpose of this paper is to present the results of an examination of the nature and magnitude of the air damping exhibited by rigid two- and three-dimensional shapes oscillating in a variable pressure environment. Circular and rectangular panels, and a sphere and cylinder were attached to cantilever springs and the free decay of an induced oscillation was studied at pressure levels from atmospheric to 4×10^{-2} torr. Data are presented to show the effect of pressure, vibratory amplitude, shape, and surface area on the air damping of the models.

APPARATUS AND PROCEDURE

Apparatus

The test program and subsequent data reduction were directed toward the isolation and examination of the effects of pressure, amplitude, shape, and area on the air damping of common shapes oscillating in a direction perpendicular to their principal surface. A study of the free decay characteristics was deemed most expedient for examining the effects of these variables independently as well as in combination. The models used in the majority of the tests are shown in figure 1. The disks and rectangular panels with surface areas of 15,

30, and 45 square inches as well as the sphere and cylinder having projected areas of 30 square inches were subjected to vibration at various pressure levels and amplitudes within a bell jar vacuum system.

The oscillation was provided by the cantilever spring system shown in figure 2. The beam, machined from a single piece of stainless steel, had a relatively large foot for mounting to a rigid base plate and a T-section at the tip for attaching the models. In all cases a frequency of 3.8 cps was maintained by adding small tuning masses to the T-section. The excitation was provided by the spring-loaded solenoid. When energized, the slug imparted a static deflection to the beam and upon removal of the current the slug was retracted by the spring. The ensuing oscillation was sensed by means of a strain gage attached to the root of the beam. The system as shown was enclosed by a bell jar capable of maintaining pressure levels between atmospheric and 4×10^{-2} torr. Additional tests were conducted at atmospheric pressure to better define the dependency of damping on panel area. Nine rectangular panels having surface areas ranging from 12 to 39 square inches were studied using the beam system described above and, in addition, three larger panels having areas of 71.3, 128, and 220 square inches were studied using a larger beam also having a tuned frequency of 3.8 cps.

Procedure

The damping characteristics of the beam alone, tuned to 3.8 cps, were studied initially followed by an examination of the damping of the beam-model system. The procedure was essentially the same in each case. The chamber, when used, was pumped down to the desired pressure level, and for all but the lowest pressure (4×10^{-2} torr), the pump was shut down while the test points were taken. The beam was then deflected, released, and damping of the oscillation

measured at various positions along the envelope. The damping was measured by an electronic dampometer and specified in terms of the logarithmic decrement,

$$\delta = \frac{1}{n} \log \frac{x_0}{x_n} \qquad (1)$$

PRESENTATION AND DISCUSSION OF RESULTS

General

For purposes of this investigation, the logarithmic decrement is physically interpreted as the ratio of the energy lost per cycle to twice the total energy,

$$\delta = \frac{\Delta E}{2E} \qquad (2)$$

as discussed in reference 1. For the system under study, the measured decrements include losses due to the beam (hysteresis, joint friction, air damping, etc.) as well as the air damping of the model or

$$\delta = \frac{\Delta E_a + \Delta E_b}{2E} = \delta_a + \delta_b \qquad (3)$$

The air damping attributed to the attached model δa is obtained by subtracting the beam damping $\frac{\Delta E_b}{2E}$, measured in a separate test under identical conditions, from the total measured decrement. These decrements are presented in terms of the variables of interest.

In examining the results, the nature of the resistive or damping forces may be inferred by comparing the measured decrements to those calculated for a single-degree-of-freedom system subjected to known loadings. If, for example, the forces are directly proportional to the velocity (often referred to as viscous) the energy loss per cycle ΔE would equal the work done by the dissipative force, or

4

$$\Delta E = \int_c X \, dx = \int_c c\dot{x} \, dx \qquad (4)$$

where the velocity is very nearly

$$\dot{x} = x_o\omega \cos \omega t \qquad (5)$$

if the system is lightly damped. Integrating equation (4) and dividing the result by twice the maximum energy of the cycle, or

$$2E = Mx_o^2\omega^2 \qquad (6)$$

yields a decrement

$$\delta = \frac{\Delta E}{2E} = \frac{\pi c}{M\omega} \qquad (7)$$

Thus in the case of viscous damping the decrement is independent of the amplitude and inversely proportional to the frequency.

Likewise a panel subjected to forces proportional to velocity squared will have a decrement of the form

$$\delta = \frac{8}{3} \frac{cx_o}{M} \qquad (8)$$

which is a linear function of amplitude and independent of frequency. These two types of damping forces, viscous and velocity squared, are of particular interest because of their common occurrence in steady-state aerodynamics.

Beam Damping

The damping associated with the fundamental mode of oscillation of the cantilever beam, tuned to 3.8 cps, is presented in figure 3. These data served as a tare for obtaining the air damping from the measured total damping values. The damping factors, in terms of the logarithmic decrement δ, are shown as a

5

function of the pressure for several different tip amplitudes. The tip amplitudes shown are the average tip displacement during the damping measurement. In this case, as well as those to follow, the data points represent an average of five or more measured values. The total damping associated with the beam exhibits a near linear dependency on pressure in the range between atmospheric pressure and 100 torr. Below 100 torr the damping factors deviate from this linear pressure relationship and approach values at 4×10^{-2} torr which are most probably due to the internal hysteresis and joint friction.

Total Damping of Beam-Model System

A typical sample of the data, as recorded, is shown in figure 4 to illustrate the magnitude of the beam damping relative to the total damping. The total damping recorded for the 30-square-inch rectangle mounted on the tip of the beam is presented as a function of pressure and amplitude. The amplitudes refer to the deflection of the center of the panel during the damping measurement and correspond to the beam tip deflections shown in figure 3. It is interesting to note the significant increase in the system damping with the addition of the panel. For example, an increase in damping by a factor of approximately five is noted in the high-pressure region. As the pressure is decreased, the values of damping converge to the values measured for the beam alone in the low-pressure region. This indicates that no extraneous damping is introduced into the system with the addition of the panel and thus the additional damping may be attributed to the air resistance.

Damping of Two-Dimensional Models

Effect of pressure.- The dependency of the air damping on the pressure environment is presented in figure 5. The air damping, obtained by subtracting

the beam damping from the total damping at corresponding pressures and amplitudes, is shown for the 30-square-inch rectangle. The damping factor exhibits a linear dependency on the pressure, and thus density, throughout the range examined. A strong dependency of the damping on the amplitude is also noted, indicating the presence of a nonlinear damping phenomena. Identical trends were noted in the other panels of 15, 30, and 45 square inches and thus these data will be presented in a subsequent section on area and shape.

Effect of amplitude.- The variation of damping with amplitude for the 30-square-inch rectangle is presented in figure 6. The trends existing in this case are again representative of the results obtained for the other two-dimensional models. For the range of amplitude examined, the damping is a near linear function of panel deflection. Because of this linear dependency, the damping is apparently of the velocity squared type as previously discussed. Thus the resistance force is proportional to the dynamic pressure ρU^2 as would be found in the case of a panel immersed in a steady stream of incompressible fluid. It should be noted that an extension of the faired lines will not intersect the origin. It is probable that in the amplitude range below 0.1 inch the forces become more viscous in nature and therefore the amplitude dependency or slope of the curve is reduced.

Effect of shape.- The effects of panel shape were examined by comparing the damping factors associated with the rectangles and disks of 15, 30, and 45 square inches. In figure 7 the decrements, measured over a wide range of pressure and amplitude, are presented as a function of the parameter $\rho x/M$ where ρ is the density of the air within the chamber, x is the amplitude of the panel, and M is the effective mass of the system located at the center of the panel. The symbols indicate the pressure levels at which the measurements

were taken. The decrement is a linear function of the parameter $\rho x/M$ which is indicative of velocity squared damping (eq. 8). For a particular area, $\delta = \frac{k\rho x}{M}$ where k is the slope of the curve associated with each configuration. In comparing the results of the disk and rectangle, the slopes of the curve k are seen to be independent of shape.

Effect of area.- As shown in figure 7, the damping increases with panel area but at a much greater rate than one to one. To examine the damping-area relationship in detail, 9 rectangular panels having surface areas ranging from 12 to 39 square inches were attached to the beam and studied at atmospheric pressure. In addition, three panels having surface areas of 71.3, 128, and 220 square inches were studied using a larger beam to further extend the range of area. The results of this study are summarized in figure 8 where the parameter $\frac{\delta M}{\rho x}(=k)$ is shown for each area. The data of figure 7 are indicated by the squared symbols. Results indicate that $\delta = 22\frac{\rho x A^{4/3}}{M}$, the exponent $4/3$ being determined from the slope of the curve. It appears that within the range of variables covered in these tests, the above relationship can be used for obtaining the variation of air damping with changes in environment.

Limited tests were also conducted within the vacuum system using a beam having a tuned frequency of 21.2 cps and panels with surface areas ranging from 12 to 45 square inches. Results of these tests verify the functional relationship observed in the low-frequency case, i.e., $\delta = \frac{K\rho x A^{4/3}}{M}$. For amplitudes above 0.1 inch, a constant of proportionality K of 22 appears adequate for predicting the damping. Below 0.1 inch, the damping ceases to be a linear function of amplitude as was the case for the low-frequency data and cannot be adequately represented by the suggested empirical relationship. It may also be noted that the damping values at these low amplitudes are substantially

8

smaller than those associated with the structural damping and it becomes increasingly difficult to accurately ascertain the true contributions of the surrounding air to the overall damping of the system.

Damping of Three-Dimensional Models

Sphere.- The problem of sphere performing pendulum oscillations of small amplitude in an incompressible viscous fluid has been examined theoretically by Lamb, reference 2. The derivation of the resultant force acting on the spherical surface yields a force component which is linearly proportional to and in opposition to the velocity as follows

$$X = 3\pi\rho a^3 \omega \left(\frac{1}{\beta a} + \frac{1}{\beta^2 a^2} \right) U \tag{9}$$

where

X   force in opposition to velocity

ρ mass density of fluid

a   radius of sphere

ω circular frequency of oscillations

$\beta = (\omega/2\nu)^{1/2}$

ν kinematic viscosity

U   velocity

When substituted into equation (7),

$$\delta = \frac{\pi c}{M\omega} = \frac{\pi}{M\omega} \left(\frac{X}{U} \right) \tag{10}$$

the resulting decrement is

$$\delta = \frac{3\pi^2 \rho a^3}{M} \left(\frac{1}{\beta a} + \frac{1}{\beta^2 a^2} \right) \tag{11}$$

The validity of this relationship is shown in figure 9 where the damping of the sphere, measured at several amplitudes, is presented as a function of pressure. The data are independent of amplitude, proportional to the square root of the density and are in good agreement with the theoretical curve.

Cylinder.- A similar theoretical treatment for a cylinder is presented in reference 3. The viscous damping force for a cylinder of high length to radius vibrating normal to its length is

$$X = \pi a^2 \rho l \omega \left(\frac{2}{\beta a} + \frac{1}{\beta^2 a^2} \right) U \qquad (12)$$

where a and l are the radius and length of the cylinder, respectively, and the other symbols are as previously defined. The resulting decrement for the cylinder is

$$\delta = \frac{\pi^2 a^2 \rho l}{M} \left(\frac{2}{\beta a} + \frac{1}{\beta^2 a^2} \right) \qquad (13)$$

The theoretical results are shown in figure 10 along with the data measured for the cylinder. In the region of low amplitude, the theory is in excellent agreement with the experimental results. At higher amplitudes, however, the decrement appears somewhat high possibly due to end effects or flow separation.

<div align="center">CONCLUSIONS</div>

Within the range of variables considered in this investigation the following conclusions are noted:

(1) For systems having a relatively large area to mass ratio, the magnitude of the air damping may greatly exceed the damping attributed to all other sources. Values of air damping, an order of magnitude greater than the structural damping, were observed during these tests.

10

(2) The damping factors associated with vibrating panels exhibit a near linear dependency on pressure and vibratory amplitude, which indicates the presence of velocity squared damping or more specifically damping forces proportional to the dynamic pressure.

(3) The damping factors associated with panels were found to be independent of shape and proportional to the product of the density, amplitude, and area raised to the 4/3 power, divided by the vibratory mass, i.e., $\delta = \dfrac{K \rho x A^{4/3}}{M}$.

(4) The damping factors associated with the sphere are essentially proportional to the square root of the density, independent of vibratory amplitude, and in good agreement with available theory based on viscous damping forces.

(5) At low amplitude the cylinder exhibits damping factors in excellent agreement with those predicted by viscous theory. At higher amplitudes the damping exceeds theoretical predictions - possibly due to end effects or flow separation.

REFERENCES

1. Thompson, William T.: Mechanical Vibrations. (Second Edition, Prentice-Hall, 1953.) Pages 55-59.

2. Lamb, Horace: Hydrodynamics. (Sixth Edition, Dover Publications, 1945.) Page 644.

3. Stokes, G. G.: Cambridge Philosophical Society Transactions, 9: 8-106 (1851).
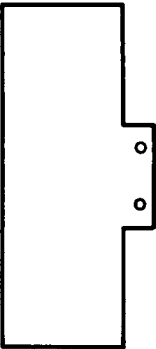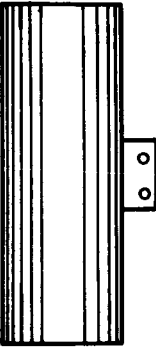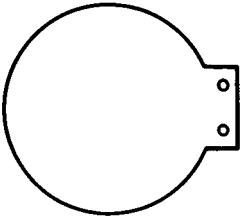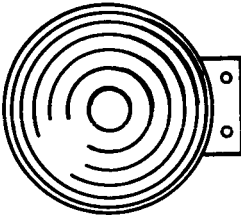
	2-D MODELS AREA, IN.²	3-D MODELS PROJECTED AREA, IN.²
	12 – 45	30
	15, 30 AND 45	30

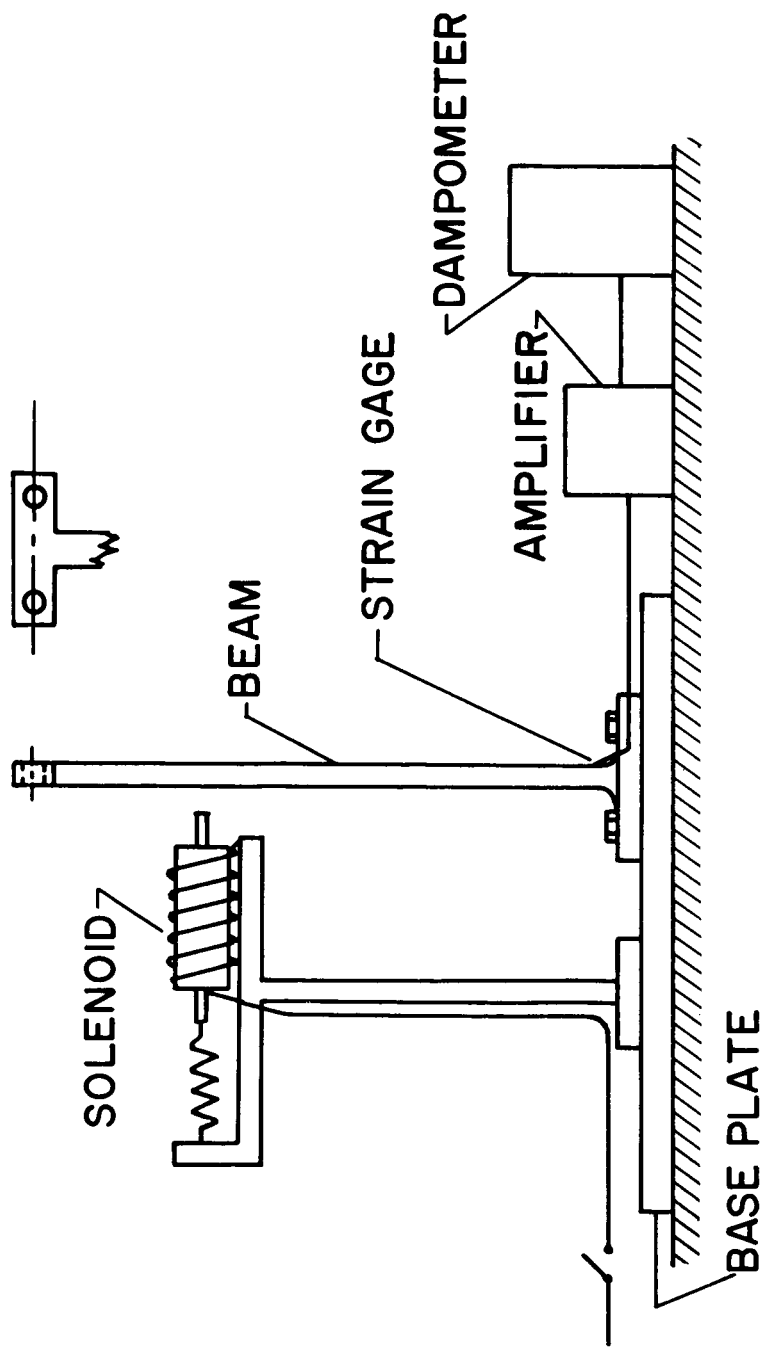Figure 1.- Damping models.

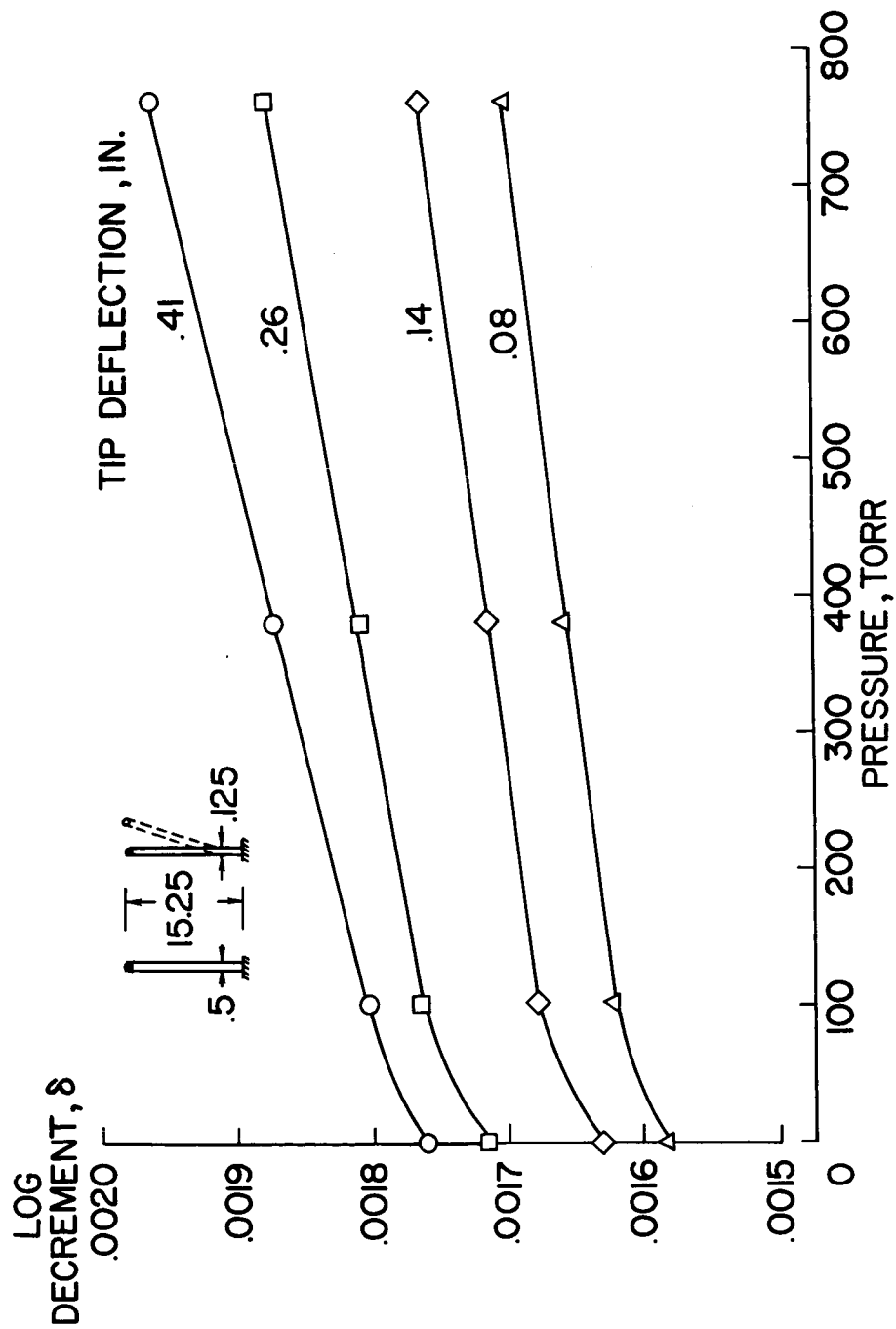Figure 2.- Test apparatus and instrumentation.

NASA

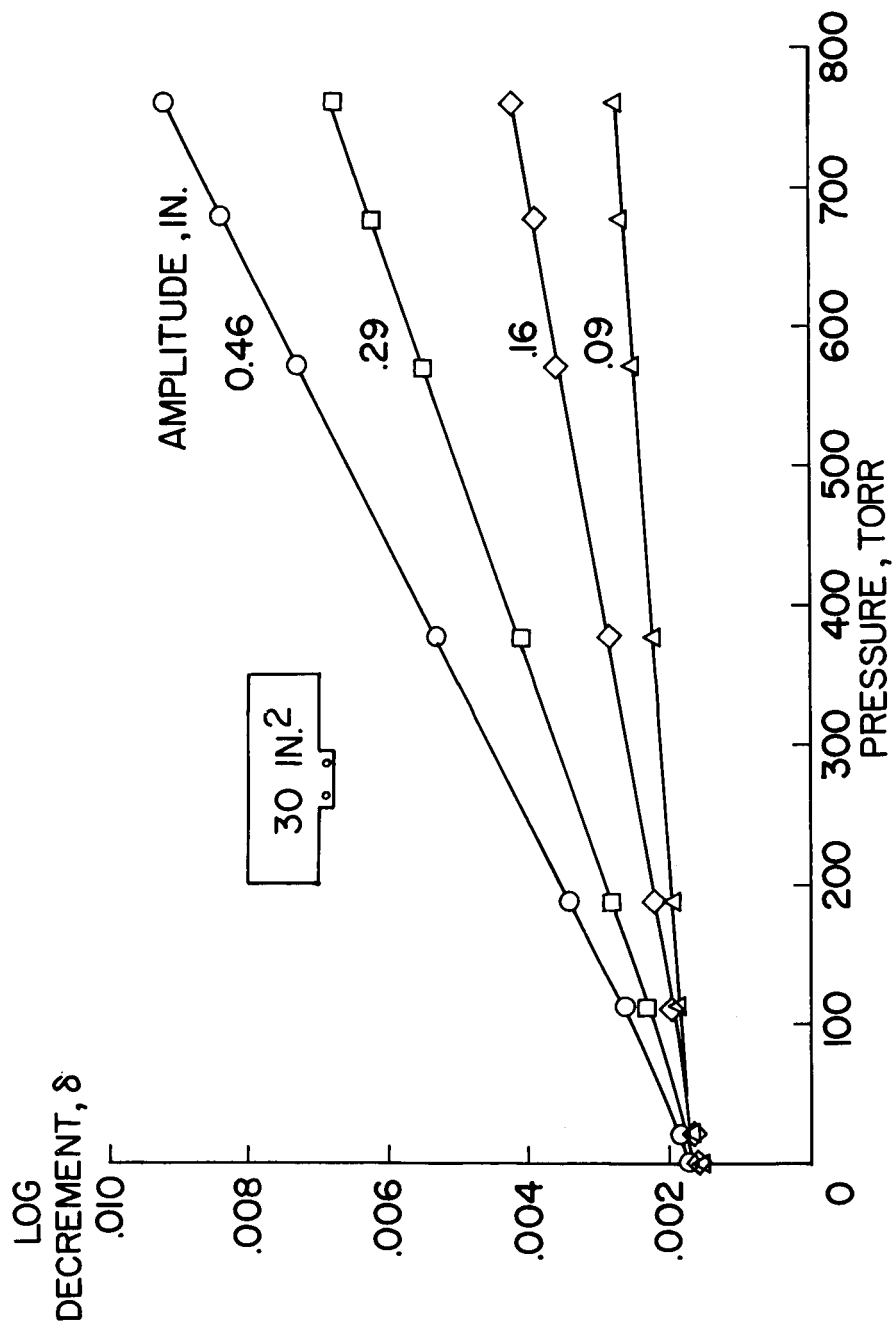Figure 3.- Variation of beam damping with pressure.

NASA

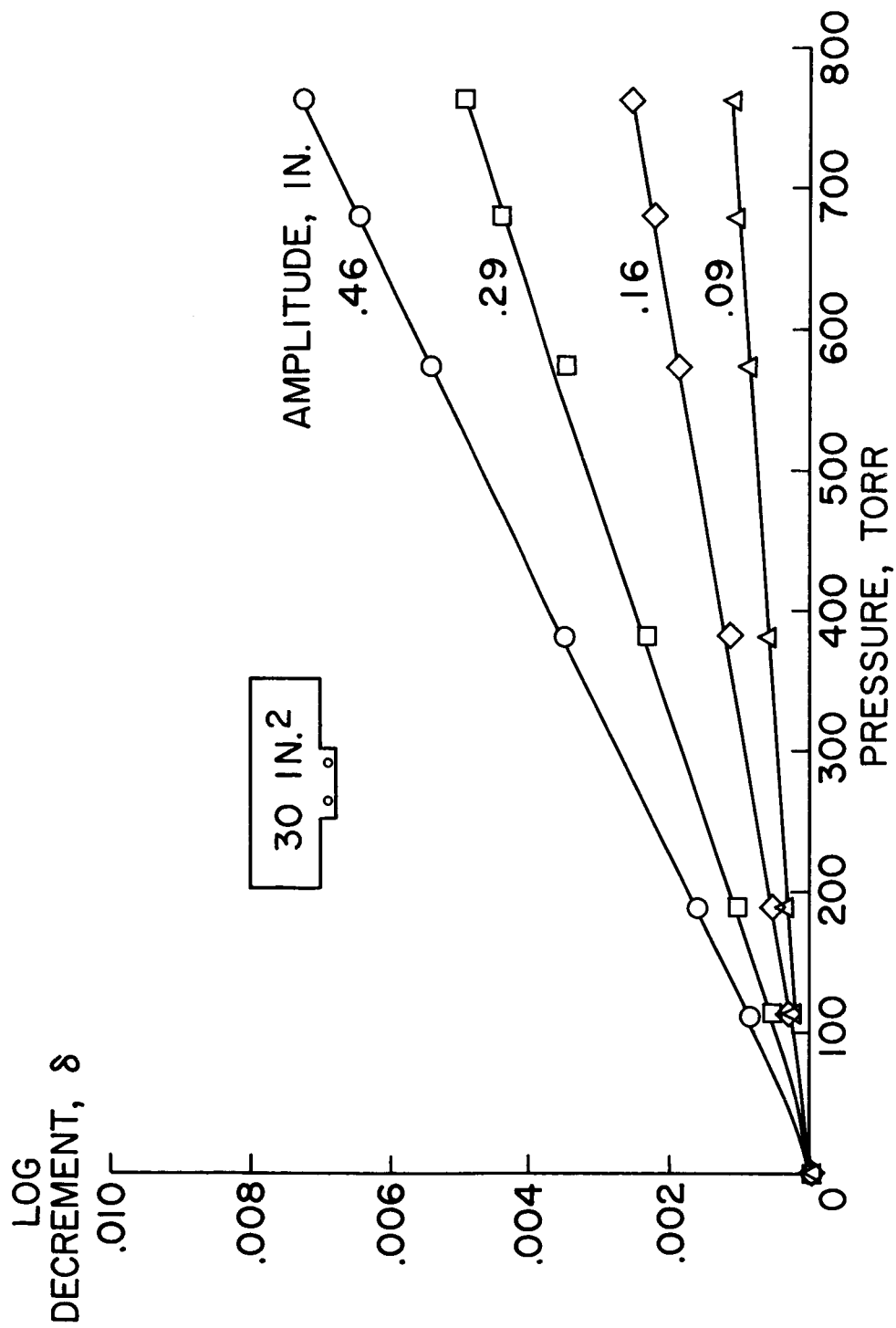Figure 4.- Variation of total damping with pressure.
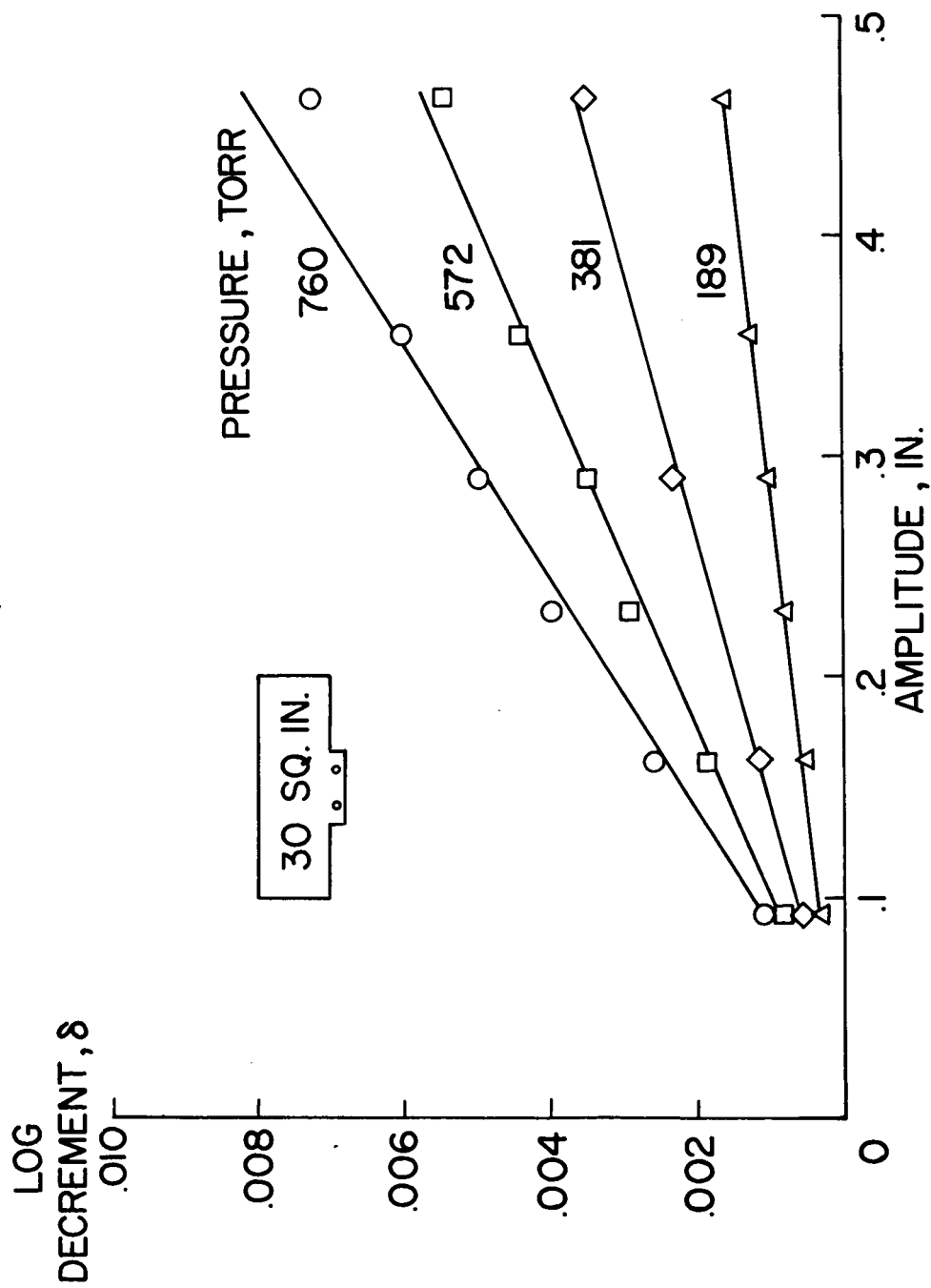
Figure 5.- Variation of air damping with pressure.
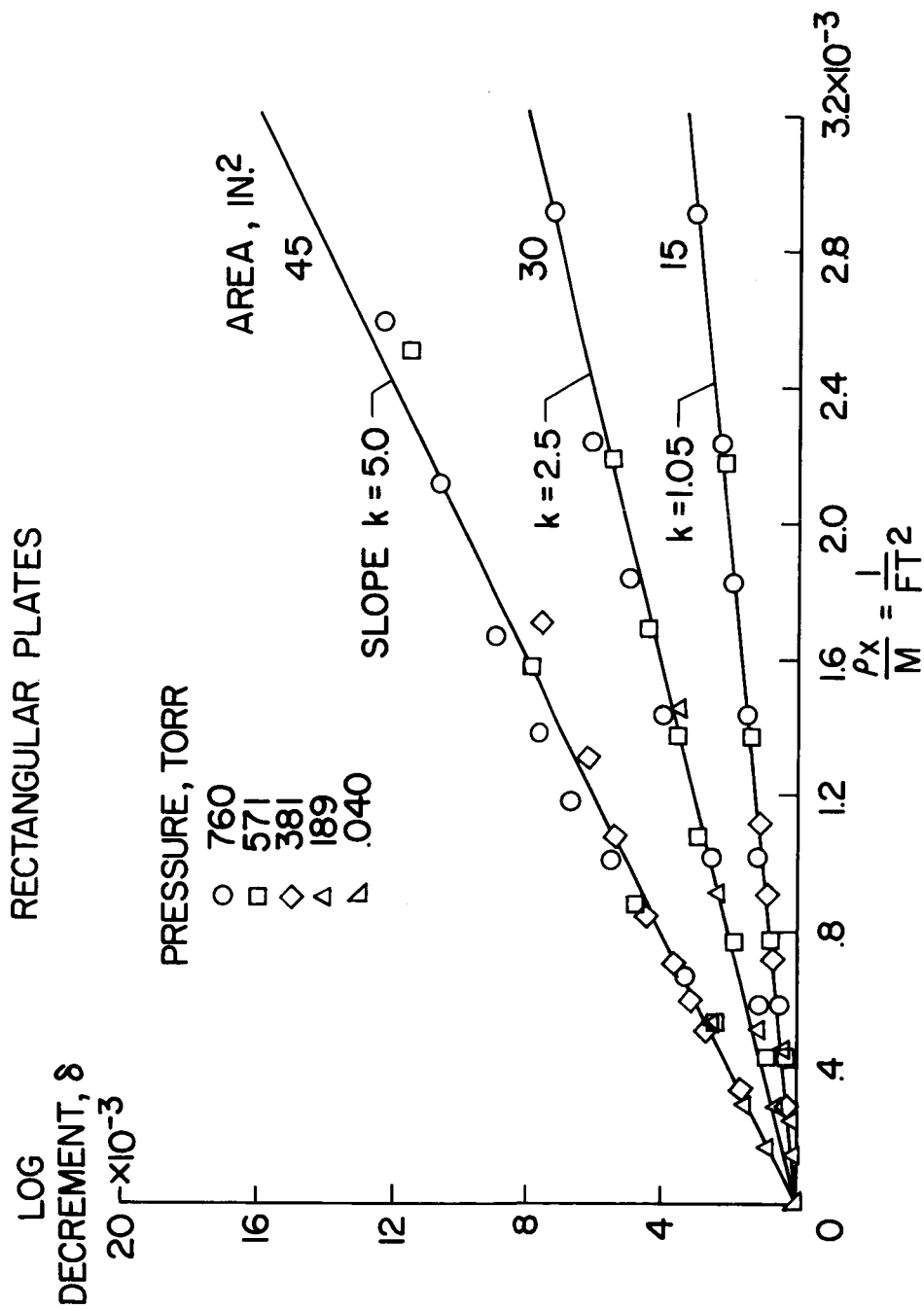
Figure 6.- Variation of air damping with amplitude.

NASA

Figure 7.- Variation of air damping with $\rho x/M$.

NASA

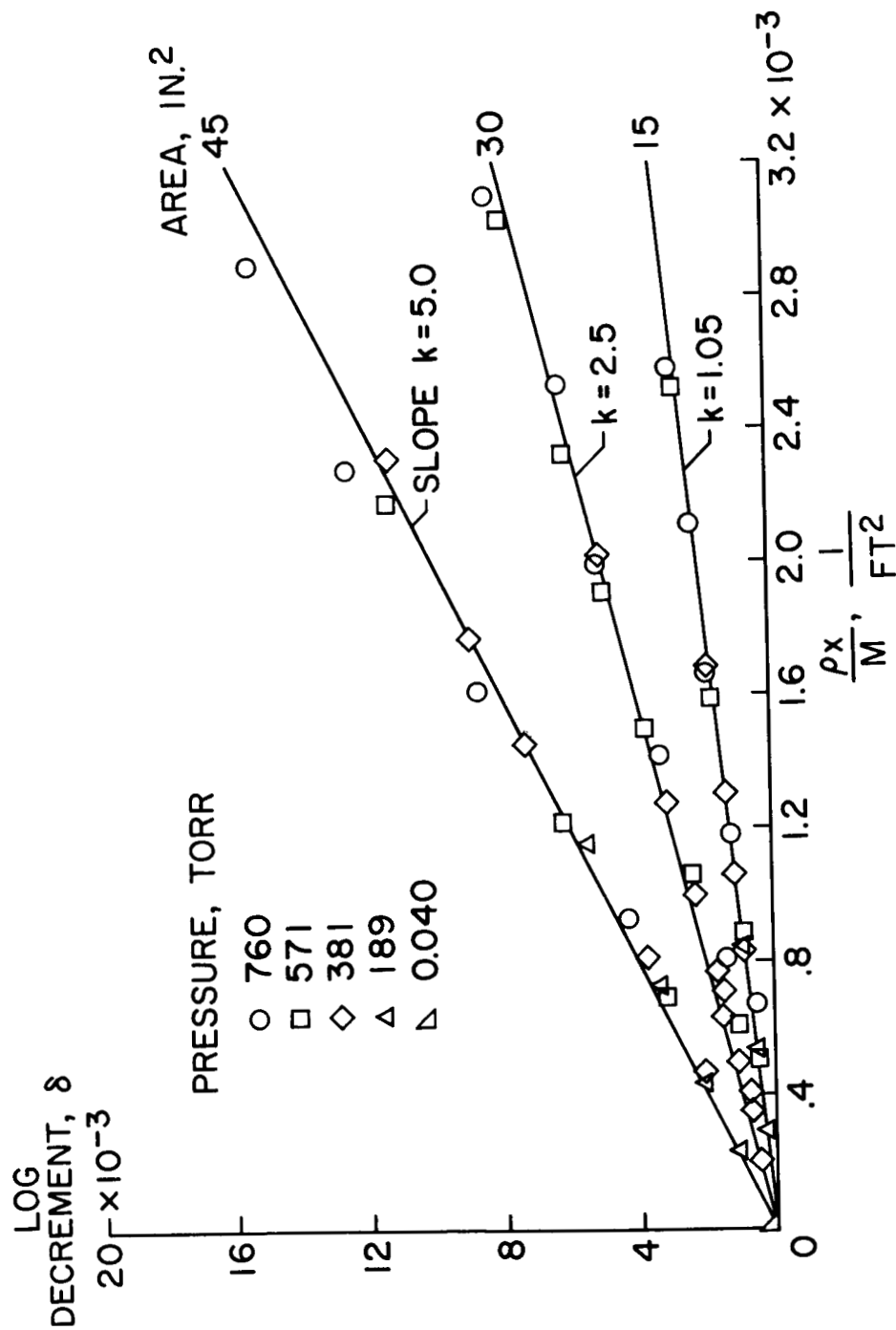Figure 7.- Concluded.

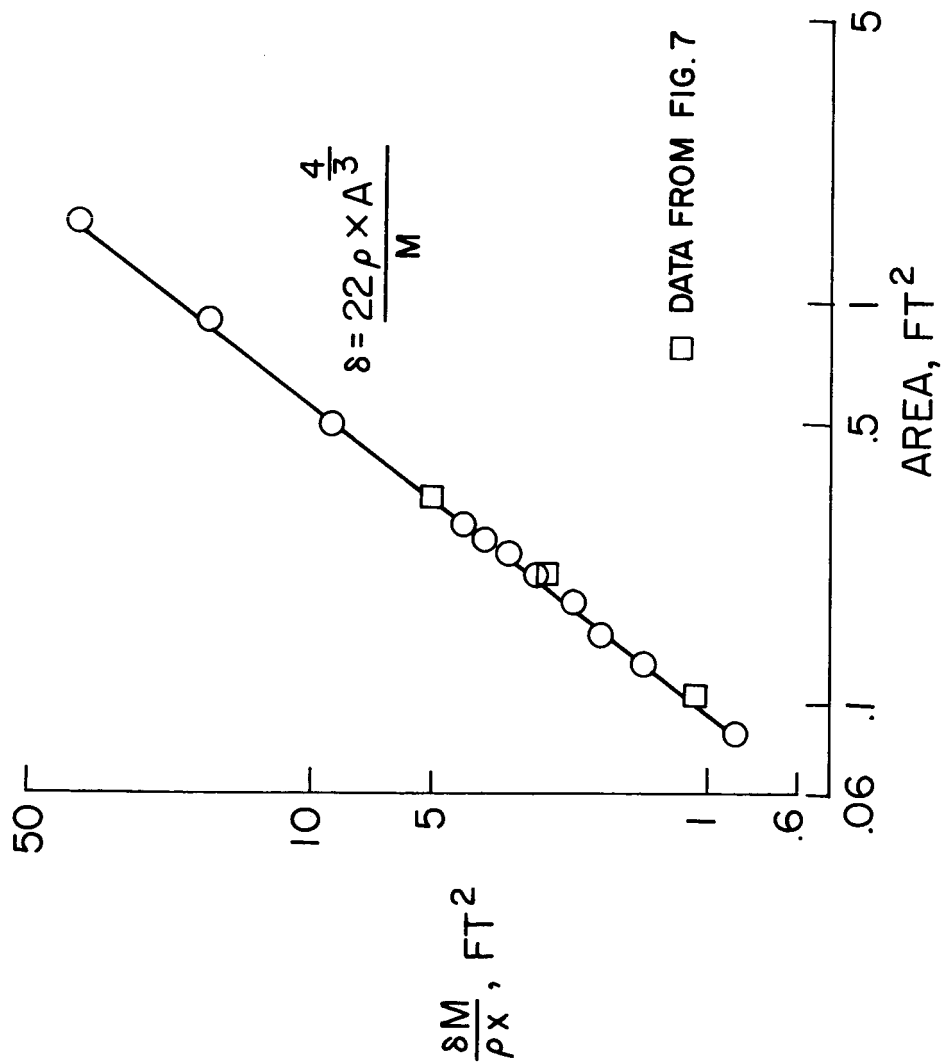Figure 8.– Variation of air damping with area for plates.

NASA

SPHERE

EXPERIMENTAL

THEORETICAL

AMPLITUDE, IN.

O .51
□ .32
◇ .18
△ .10

LOG
DECREMENT, δ

.002

.001

.01

PRESSURE, TORR

0   100   200   300   400   500   600   700   800
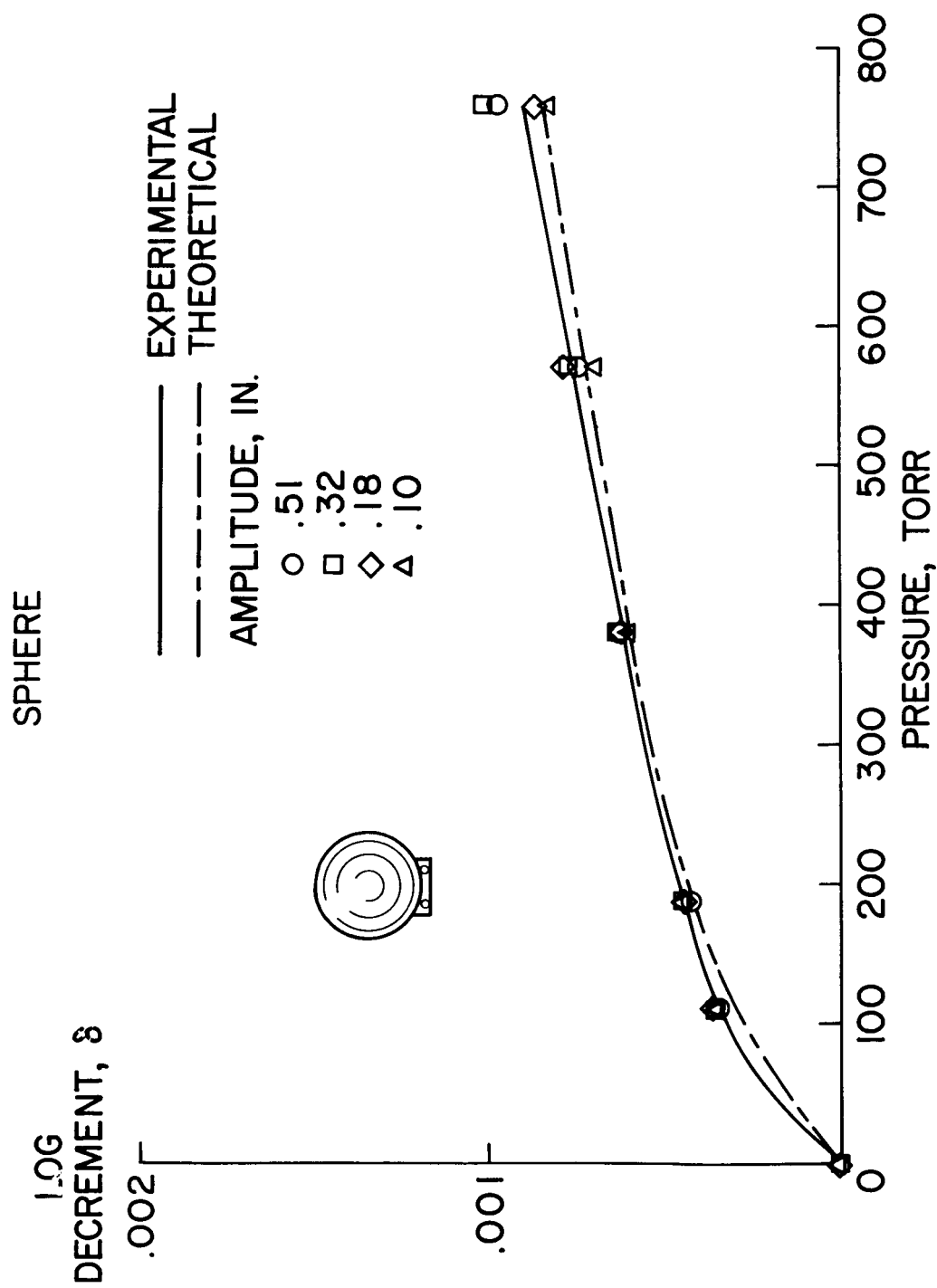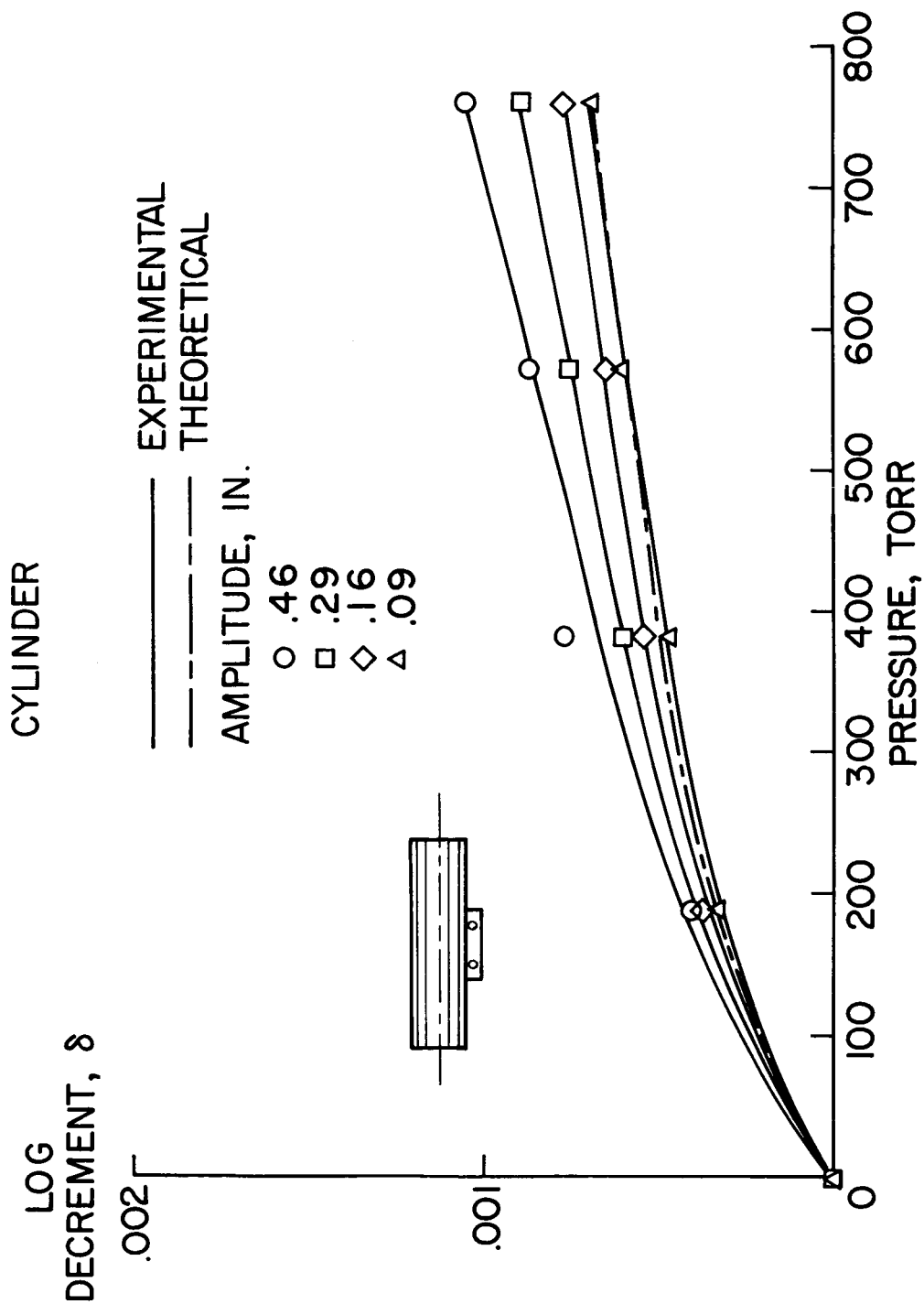
Figure 9.- Variation of air damping with pressure.

Figure 10.— Variation of air damping with pressure.